Improvement of Multi-Satellite Real-Time Precipitation Products for Ensemble Streamflow Simulation in a Middle Latitude Basin in South China

**Shanhu Jiang · Liliang Ren · Yang Hong · Xiaoli Yang ·
Mingwei Ma · Yu Zhang · Fei Yuan**

Abstract The real-time availability of several satellite-based precipitation products has recently provided hydrologists with an unprecedented opportunity to improve current hydrologic prediction capability for vast river basins, particularly for ungauged regions. However, the accuracy of real-time satellite precipitation data remains uncertain. This study aims to use three widely used real-time satellite precipitation products, namely, TRMM Multi satellite Precipitation Analysis real-time precipitation product 3B42 (TMPA 3B42RT), Precipitation Estimation from Remote Sensing Information using Artificial Neural Network (PERSIAN), and NOAA/Climate Precipitation Center Morphing Technique (CMORPH), for ensemble stream flow simulation with the gridded xinanjiang (XAJ) model and shuffled complex evolution metropolis (SCEM-UA) algorithm in the middle-latitude Mishui basin in South China. To account the bias of the satellite precipitation data and consider the input uncertainty, two different methods, i.e. a precipitation error multiplier and a precipitation error model were introduced. For each precipitation input model, the posterior probability distribution of the parameters and their associated uncertainty were calibrated using the SCEM-UA algorithm, and 15,000 ensemble stream flow simulations were conducted. The simulations of the satellite precipitation data were then optimally merged using the Bayseian model averaging (BMA) method. The result shows that in Mishui basin, the three sets of real-time satellite precipitation data largely underestimated rainfall. Streamflow simulation performed poorly when the raw satellite precipitation data were taken as input and the model parameters were calibrated with gauged data. By implementing the precipitation error multiplier and the precipitation error model and then recalibrating the model, the behavior of the simulated stream flow and calculated uncertainty boundary were significantly improved. Furthermore, the BMA combination of the simulations from the three datasets resulted in a significantly better prediction with a remarkably reliable uncertainty boundary and was comparable with the simulation using the post-real-time bias-corrected research quality TMPA 3B42V7.

S. Jiang · L. Ren (✉) · X. Yang · M. Ma · F. Yuan
State Key Laboratory of Hydrology-Water Resources and Hydraulic Engineering, College of Hydrology and Water Resources, Hohai University, Nanjing, China
e-mail: njRLL9999@126.com

Y. Hong · Y. Zhang
School of Civil Engineering and Environmental Sciences and School of Meteorology, University of Oklahoma, Norman, OK, USA

The proposed methodology of bias adjustment, uncertainty analysis, and BMA combination collectively facilitates the application of the current three real-time satellite data to hydrological prediction and water resource management over many under-gauged basins. This research is also an investigation on the hydrological utility of multi-satellite precipitation data ensembles, which can potentially integrate additional more satellite products when the Global Precipitation Measuring mission with 9-satellite constellation is anticipated in 2014.

Keywords Satellite precipitation · Error adjustment · Ensemble streamflow simulation · Uncertainty analysis · Hydrological model · Bayesian model averaging

1 Introduction

Precipitation is one of the most important and active physical process in the hydrologic cycle, and its temporal and spatial distribution significantly affect the land surface hydrological fluxes and states (Gottschalck et al., 2005; Su et al., 2008; Kidd and Huffman., 2011). Obtaining accurate and reliable precipitation data is thus very important for the real-time monitoring of local, regional, and global disasters as well as hydrologic process simulation and climate change research (Jiang et al. 2010; Yu et al. 2011). Among the three primary sources of precipitation observations (i.e., surface networks, ground-based radar, and satellite remote sensing retrieval), satellite remote sensing retrieval data can provide complete coverage of the global precipitation map (Kucera et al., 2013). A number of new global high-resolution satellite-based precipitation products have recently been made operationally available, including the TRMM Multi satellite Precipitation Analysis (TMPA) 3B42 (Huffman et al. 2007), NOAA/Climate Precipitation Center Morphing Technique (CMORPH) (Joyce et al., 2004), Precipitation Estimation from Remote Sensing Information using Artificial Neural Network (PERSIAN) (Sorooshian et al., 2000), Precipitation estimation from remotely sensed imagery using Artificial Neural Network-Cloud Classification System (PERSIAN-CCS) (Hong et al. 2004), Global Satellite Mapping of Precipitation (GSMaP) (Kubota et al., 2007) and so on. These high-resolution satellite precipitation products can be divided into two types: post-real-time research satellite precipitation product (e.g., TMPA 3B42V7, hereinafter referred to as 3B42V7) and real-time pure satellite precipitation products (e.g., TMPA 3B42RT, hereinafter referred to as 3B42RT). These products provide new data sources for hydrological research and applications. Thus, facilitating the full-scale application of these satellite precipitation products in monthly, daily, and sub-daily hydrological operations is important.

Numerous studies have evaluated the accuracy and hydrological simulation utility of the available satellite precipitation products. These studies highlighted that different satellite precipitation products have variable accuracy and distinct hydrological utility in different regions (Stisen and Sandholt 2010; Behrangi et al., 2011; Yong et al., 2012; Jiang et al., 2012; Li et al., 2013; Xue et al., 2013). Moreover, a post-real-time gauge bias-adjusted satellite precipitation product (e.g., 3B42V7) usually has higher accuracy than a real-time pure satellite precipitation product (e.g., 3B42RT). However, in practical application, the timeliness of a satellite precipitation product is critical to real-time disaster monitoring. Thus, a new challenge has been presented by requirement for the bias adjustment of real-time pure satellite precipitation products and the improvement of the stream flow simulation by merging the information from different real-time pure satellite precipitation products. Hong et al. (2006) assumed the error of the satellite precipitation product to be a nonlinear function of rainfall space-time integration scale, rain intensity, and sampling frequency to assess the influence of precipitation estimation error on the uncertainty of hydrological response and to determine the accuracy

confidence interval. Strauch et al. (2012) used different precipitation data ensembles for stream flow simulation uncertainty analysis and found that ensemble modeling with multiple precipitation inputs can considerably increase the level of confidence in simulation results. Gebregiorgis and Hossain (2011) merged individual satellite precipitation products according to their prior hydrologic predictability and indicated that the merging method can yield a more superior product for stream flow prediction. Although these studies have conducted on the bias adjustment, satellite ensemble generation, and stream flow simulation using the available real-time satellite precipitation products, these works still have to be supplemented.

Thus, this study focus on an integrated framework of bias adjustment, uncertainty analysis, and ensemble combination collectively facilitates the application of the current three real-time satellite data to hydrological prediction and water resource management over many under-gauged basins. There are three main steps: (1) adjust the bias of the three most widely used global high-resolution real-time pure satellite precipitation products (3B42RT, PERSIAN, and CMORPH) using two different methods: a precipitation error multiplier and a precipitation error model; (2) perform 15,000 ensemble stream flow simulations using the gridded Xinanjiang model (hereinafter referred to as XAJ, Zhao et al., 1992) and the shuffled complex evolution metropolis algorithm (SCEM-UA, Vrugt et al., 2003) for each precipitation input model; and (3) optimally merge the simulations from the three sets of real-time satellite precipitation data using the Bayesian model averaging method (BMA). The BMA-combined results of the three real-time pure satellite precipitation products are compared with the gauge-based and 3B42V7-based simulation to verify the effectiveness of the bias adjustment, uncertainty analysis, and BMA combination method.

The remainder of this paper is organized as follows: Section 2 introduces the study area and the datasets used. Section 3 describes the detailed methodology. Section 4 discusses the simulation results of different simulation scenarios. Finally, Section 5 draws the conclusions.

2 Study Area and Data

2.1 Study Area

Mishui basin, a tributary of Xiangjiang River with a drainage area of 9,972 km^2 above the Ganxi hydrologic station, was selected as the study area (Fig. 1). The basin is located southeast of Hunan Province in South China and extends from longitudes 112.85°E to 114.20°E and latitudes 26.00°N to 27.20°N. The basin has a complex topography, with elevations ranging from 49 m to 2093 m above sea level. The land use in the basin is composed of forest and shrubs (54.4 %), grassland (33.5 %), cropland (11.8 %), and urban and water (0.3 %). The climate is a humid subtropical monsoon type, with average temperature of approximately 18.0 °C and mean annual precipitation of approximately 1,561 mm. The temporal and spatial distribution of precipitation is uneven because of atmospheric circulation and because most of the annual precipitation occurs between April and September. In these months, particularly in June, basin-wide heavy rains continuously occur, thereby resulting in floods. Mishui basin is a typical middle-latitude humid basin in China.

2.2 Data

2.2.1 Satellite Precipitation Products

The satellite precipitation products used in this study include one post-real-time research satellite precipitation product, i.e., 3B42V7, and three real-time pure satellite precipitation products, i.e., 3B42RT, CMORPH, and PERSIAN. All these satellite precipitation products are generated by
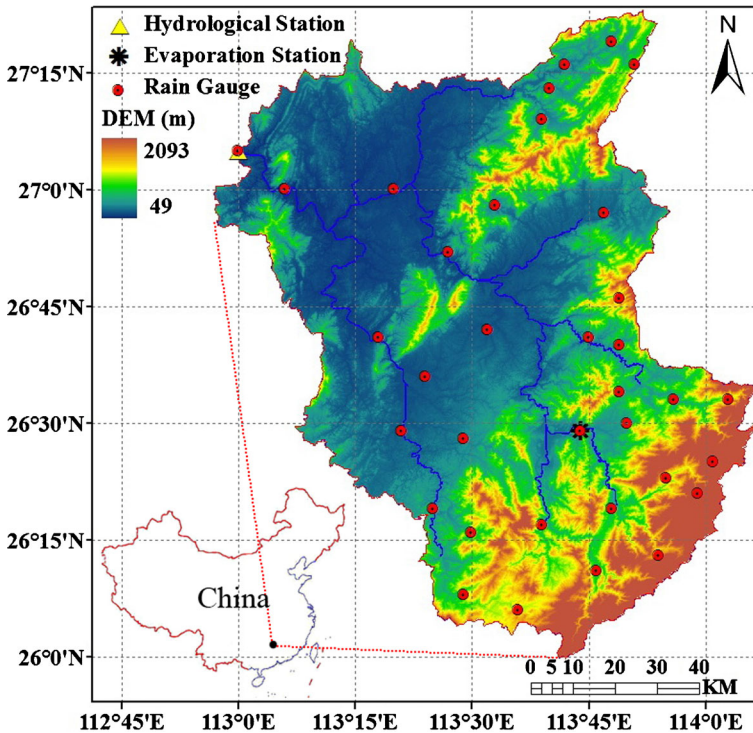
Fig. 1 Map of Mishui basin in South China

combining multi-source information from more accurate (but infrequent) microwave (MW) observations and more frequent (but indirect) infrared (IR) observations, but the data sources and retrieval algorithms are different (Bitew and Gebremichael, 2011). The TMPA method (Huffman et al., 2007) retrieves real-time precipitation through three consecutive stages: 1) polar-orbiting MW precipitation estimates are calibrated by TRMM MW estimates and then combined together, 2) geostationary IR precipitation estimates are calibrated using the merged MW precipitation to fill in gaps of the MW coverage, and 3) MW and IR data are combined to form the real-time pure satellite precipitation product (i.e., 3B42RT). The CMORPH method (Joyce et al., 2004) obtains real-time precipitation estimations from MW data but uses a tracking approach in which IR data are used to derive a cloud motion field that is subsequently used to propagate raining pixels. The PERSIAN method (Sorooshian et al., 2000) uses a neural network approach to derive the relationships between IR and MW data and is applied to the IR data to generate real-time precipitation estimates. Thus, TMPA and CMORPH products primarily rely on MW data for precipitation estimates, whereas PERSIAN primarily uses IR data. All the three satellite precipitation products are real-time versions. By contrast, TMPA products provide a post-real-time research version precipitation estimate, i.e., 3B42V7. 3B42V7 uses the TRMM combined instrument (includes the TRMM precipitation radar and TRMM MW) product as a calibrator of the MW estimates from other satellites. Additionally, the 3B42V7 estimate adjusts its bias based on monthly rain gauge observations (Huffman et al., 2007). 3B42V7 has been identified as the most accurate among all available satellite precipitation products. The resolution of the satellite precipitation products used in this study are 0.25 and 3 hourly, although finer resolutions are also available for CMORPH and PERSIAN. The 3-hourly satellite precipitation products were aggregated to produce the accumulated daily precipitation for daily stream flow simulation.

2.2.2 Gauged Precipitation and Discharge Data

The observed daily precipitation data for 2003 to 2008 were derived from 35 rain gauge stations in Mishui basin using roughly two rain gauges within one 0.25 grid. For the same period, daily stream flow and potential evapotranspiration data were collected from the Ganxi hydrologic station and Wulipai evaporation station, respectively. The inverse distance weighting (Bartier and Keller, 1996) of the three nearest rain gauges was used to obtain the spatially distributed precipitation database of Mishui basin. The 30 arc-second global digital elevation model data were obtained from the U.S. Geological Survey, whereas the vegetation-type data were obtained from the International Geosphere-Biosphere Program.

3 Methodology

3.1 Simulation Scenarios

For the post-real-time research satellite precipitation product 3B42V7, the XAJ model parameters were calibrated based on the rain gauge precipitation measurements. The period from 2003 to 2005 was selected as the calibration period, whereas that from 2006 to 2008 was selected as the validation period. The SCEM-UA algorithm was used for parameter calibration and uncertainty analysis.

For the three real-time satellite precipitation products (i.e., 3B42RT, PERSIAN, and CMORPH), rainfall was largely underestimated. The average biases of the products from 2003 to 2008 are −42.72 %, −56.80 %, and −40.81 %. The biases should be adjusted before using the products for stream flow simulation. Thus, we adopt three different cases to combine the XAJ model and SCEM-UA algorithm for stream flow simulation.

1. In case 1, the XAJ model parameters were calibrated based on the rain gauge precipitation measurements, and model runs were repeated with the three real-time satellite precipitation products as inputs. The simulations of the three real-time satellite precipitation products were then merged using the BMA method.
2. In case 2, the biases of the three real-time satellite precipitation products were adjusted using a precipitation error multiplier, and then the model parameters were recalibrated with each of the bias-adjusted satellite precipitation products as input. Finally, the simulations of the three bias-adjusted real-time satellite precipitation products were merged using the BMA method. The formula for the error multiplier is given by

$$P_e = \varphi_t \cdot P \tag{1}$$

$$\varphi_t = N(m, \sigma_m^2) \tag{2}$$

where P_e is the bias-adjusted satellite precipitation, P is the raw satellite precipitation, φ_t is a normal error multiplier with a mean value of m and a variance of σ_m^2, and t is the number of the total simulation days. In this study, the m values are determined based on the bias of each satellite precipitation. The m value range for 3B42RT is [1.73, 1.77], that for PERSIAN is [2.29, 2.33], and that for CMORPH is [1.67, 1.71]. The three satellite precipitation products have the same σ_m^2 value range of [1e-5, 1e-3]. In the model calibration, m and σ_m^2 were regarded as two model parameters, such that we can obtain the optimal values of these parameters.

(3) In case 3, the biases of the three real-time satellite precipitation products were adjusted using a simple precipitation error model. The biases of the three sets of real-time satellite precipitation data were assumed as a nonlinear function of rainfall space–time integration scale, rain intensity, and sampling frequency. The model parameters were then recalibrated with each of the bias-adjusted satellite precipitation products as input. Finally, the simulations of the three bias-adjusted real-time satellite precipitation products were merged using the BMA method. The formula for the error model is given by

$$m_e = f\left(\frac{1}{L}, \frac{\Delta t}{T}, P\right) = a \cdot \left(\frac{1}{L}\right)^b \cdot \left(\frac{\Delta t}{T}\right)^c \cdot (P)^d \tag{3}$$

$$P_e = P + m_e \cdot \varepsilon \tag{4}$$

where m_e is the basin scale bias of satellite precipitation, L is the space–time integration scale of satellite precipitation, T is the time scale of satellite precipitation, Δt is the sampling frequency of satellite precipitation, P_e is the bias-adjusted satellite precipitation, and P is the raw satellite precipitation. a, b, c, and d are the four parameters of the precipitation error model, the values of which can be estimated by comparing the estimated bias and the true bias time series for the calibration period. ε is a normal value with a mean value of m and a variance of σ_m^2. The m value range is [0.95, 1.05], and the σ_m^2 value range is [1e-5, 1e-3]. Similar to case 2, the m and σ_m^2 were regarded as two model parameters in the model calibration, such that we can determine the optimal values of these parameters.

3.2 XAJ Model

Xinanjiang model is a well-known physically based conceptual hydrological model developed by Zhao in the 1970s (Zhao, 1992). Since its development, the Xinanjiang model has been successfully and widely used in the humid and semi-humid regions of China. The runoff generation method of the Xinanjiang model has also been widely used in distributed hydro-logical models. For example, the core of the model, which describes the spatial heterogeneity of tension water and free water within a basin based on the storage capacity distribution curves, was employed by the three-layer variable infiltration capacity model. In this work, a gridded-structured Xinanjiang model for stream flow simulation was constructed. The simulation was performed by computing the runoff and dividing the runoff types within each grid. The slope and river network convergence processes were then integrated to obtain the stream flow series of the hydrologic station. The model was operated daily with a 0.25×0.25 spatial resolution from January 2003 to December 2008. The model has 16 parameters, and they were auto-matically calibrated using the SCEM-UA algorithm, which can be used for model parameter calibration and uncertainty analysis.

3.3 Parameter Calibration and Uncertainty Analysis

The SCEM-UA was built upon the principles of shuffled complex evolution (SCE-UA), an effective and efficient global optimization technique developed by Duan et al. (1994). Vrugt et al. (2003) combined the strengths of the Monte Carlo Markov Chain sampler with the concept of complex shuffling from SCE-UA to form an algorithm that not only provides the most probable parameter set, but also estimates the uncertainty associated with estimated parameters. The SCEM-UA can simultaneously identify the most likely parameter set and its

associated posterior probability distribution in every model run (Ajami et al., 2007). The SCEM-UA has been successfully used for hydrologic and climate applications, such as rainfall-runoff model parameter calibration and uncertainty analysis (Kwon et al., 2012). The detailed calculation steps of SCEM-UA can be found in the literatures Vrugt et al. (2003) and Ajami et al (2007). In this study, the initial samples and the computation times were set at 5,000 and 10,000, respectively.

3.4 Streamflow Merging Method

Bayesian model averaging (BMA) is a probabilistic scheme for model combinations that derives the consensus prediction from competing predictions using likelihood measures as model weights. BMA has previously been primarily used to generalize linear regression applications. Raftery et al. (2005) successfully applied BMA to dynamical numerical weather predictions. Duan et al. (2007) and Ajami et al. (2007) used the BMA scheme to combine multi-models for hydrologic ensemble prediction, which can develop more skillful and reliable probabilistic prediction. The advantage of the BMA is that the weights are directly bound with individual model simulation, i.e., a better performing model can receive a higher weight than a poorly performing one. A more robust and stable result can be obtained when the BMA method is used to combine different simulations. In this study, we use the BMA to merge the simulated stream flows of the three real-time satellite precipitation products. Each satellite precipitation product has its own merits in terms of capturing real rainfall events. With different satellite precipitation products as input forcing data, the hydrological model can generate various stream flow series with different accuracies. Merging the different satellite data forced stream flow simulations using the BMA method is thus considered a novel method that may generate a better, more stable stream flow series. The detailed calculation steps of the BMA method can be found in the literatures Duan et al. (2007) and Ajami et al. (2007).

3.5 Evaluation Statistics

The validation statistical indices of Nash–Sutcliffe coefficient (NSCE), relative bias (BIAS), and root mean square error (RMSE) were employed to evaluate hydrologic model performance based on the observed and simulated stream flow series. These three indices jointly measure the consistency of the simulated and observed stream flow series both in terms of temporal distribution and amount. The formula for NSCE, BIAS, and RMSE are given by

$$NSCE = 1 - \frac{\sum\limits_{i=1}^{n} (Q_{oi} - Q_{si})^2}{\sum\limits_{i=1}^{n} (Q_{oi} - \overline{Q_o})^2} \tag{5}$$

$$BIAS = \frac{\sum\limits_{i=1}^{n} Q_{si} - \sum\limits_{i=1}^{n} Q_{oi}}{\sum\limits_{i=1}^{n} Q_{oi}} \times 100\% \tag{6}$$

$$RMSE = \sqrt{\frac{1}{n} \sum\limits_{i=1}^{n} (Q_{si} - Q_{oi})^2} \tag{7}$$

where Q_{oi} is the observed runoff at time step i, Q_{si} is the simulated runoff at time step i, $\overline{Q_o}$ is the mean value of the observed stream flow values, $\overline{Q_s}$ is the mean value of the simulated stream flow values, and n is the number of simulation days.

The validation statistical indices of the containing ratio (CR), average bandwidth (B), and average deviation amplitude (D) were adopted to evaluate the prediction bounds of the hydrological models (Xiong et al., 2009). CR denotes the ratio of the number of observed stream flows enveloped by prediction bounds to the total number of observed hydrographs, expressed as a percentage. B represents the average bandwidth of the whole prediction bounds. With a certain confidence level, a small B indicates a perfect prediction bound. D denotes the actual discrepancy between the trajectories consisting of the middle points of the prediction bounds and the observed hydrograph and shows the symmetry with respect to the observed stream flows and the middle point of the prediction bounds. The formulas for CR, B, and D are given by

$$CR = \frac{n_c}{n} \times 100\% \tag{8}$$

$$B = \frac{1}{n} \sum_{i=1}^{n} (q_{ui} - q_{li}) \tag{9}$$

$$D = \frac{1}{n} \sum_{i=1}^{n} \frac{1}{2} |(q_{ui} + q_{li}) - Q_{oi}| \tag{10}$$

where n_c is the number of observed stream flows enveloped by prediction bounds; n is the total number of the observed hydrographs; q_{ui} and q_{li} are the upper and low boundaries of the prediction bounds at time step i, respectively.

4 Results and Discussion

4.1 Streamflow Simulation from Gauge Data and 3B42V7

To evaluate the stream flow simulation utility of the three real-time satellite precipitation products, the XAJ model was first calibrated using the data of 35 rain gauge stations as input in where. The calibration was processed automatically with the objective function of maximizing the likelihood function using the SCEM-UA algorithm, and the model parameters were selected within the experiential numerical range. Figure 2 shows the daily and monthly comparisons of the observed stream flow with the mean value of 10,000 simulations (when the model parameters are in convergence) and the calculated 95 % confidence interval for both the calibration and validation periods. Overall, good agreement exists between the observed and simulated stream flow series both in the daily and monthly time scales. The statistical indices, which reflect the simulated stream flow performances (with daily NSCE of 0.91 and 0.80, monthly NSCE of 0.97 and 0.91, BIAS of 0.97 % and 4.81 %, and daily RMSE of 0.32 and 0.65 mm, as well as monthly RMSE of 6.89 and 17.62 mm for the calibration period and validation periods, respectively), indicate that the XAJ model can capture key features of the observed hydrograph. The statistical indices, which reflect the reliable performance of the calculated uncertainty boundary (with daily CR of 81.20 % and 83.30 %, monthly CR of
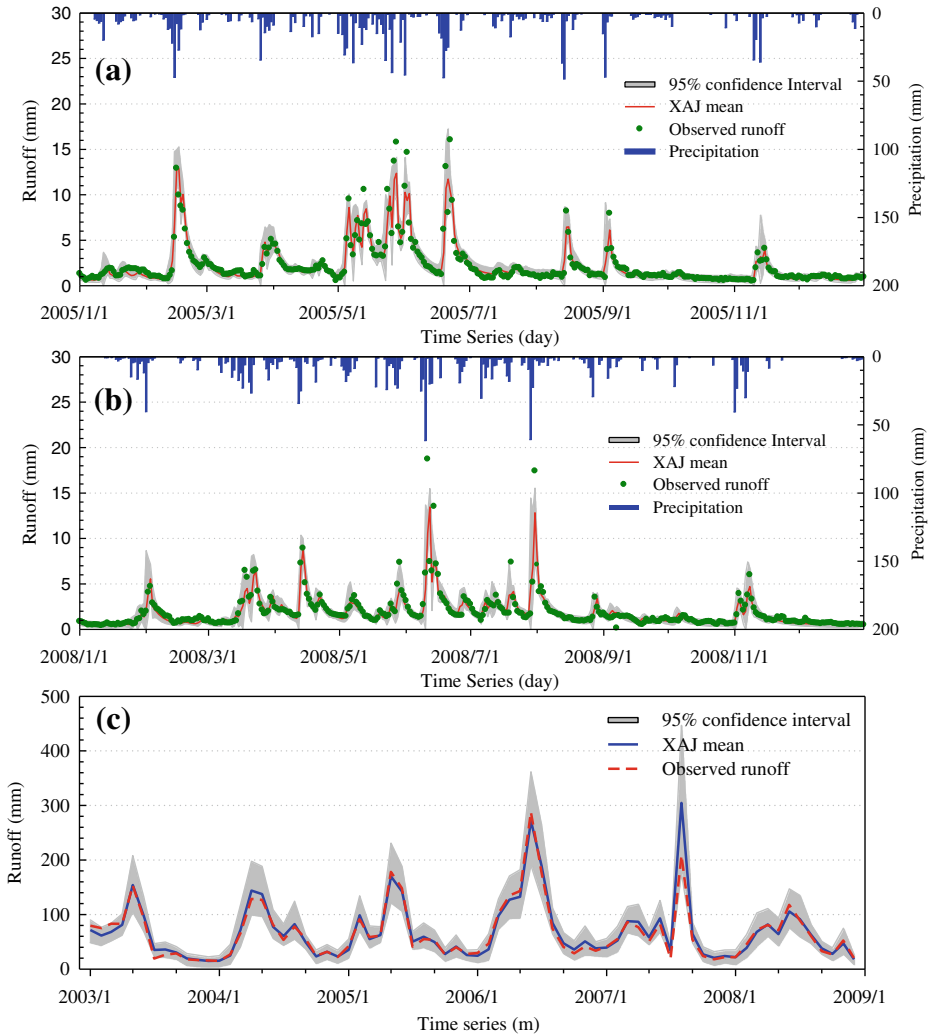
Fig. 2 XAJ model simulated runoff and calculated 95 % confidence interval based on the gauged rainfall data as input: **a** daily Calibration Period (CP) time series, **b** daily Validation Period (VP) time series and **c** monthly time series

97.22 % and 97.22 %, daily B of 1.45 and 1.82 mm, monthly B of 44.11 and 55.45 mm, and daily D of 0.43 and 0.59 mm, and monthly D of 5.79 and 8.68 mm for the calibration and validation periods, respectively), indicate that the uncertainty boundary can consistently contain the observed hydrograph.

For the 3B42V7 satellite precipitation, we use the rain gauge data calibrated XAJ model for the stream flow simulation. Figure 3 shows the daily and monthly comparisons of the observed stream flow with the mean value of 10,000 3B42V7-simulated simulations and calculated 95 % confidence interval for both the calibration and validation periods. The 3B42V7-simulated stream flow is in good agreement with the observed hydrograph. The calculated 95 % confidence interval contains most of the observed stream flow series, but at the daily time scale, some minimum and maximum values run out of the interval. The statistical indices of
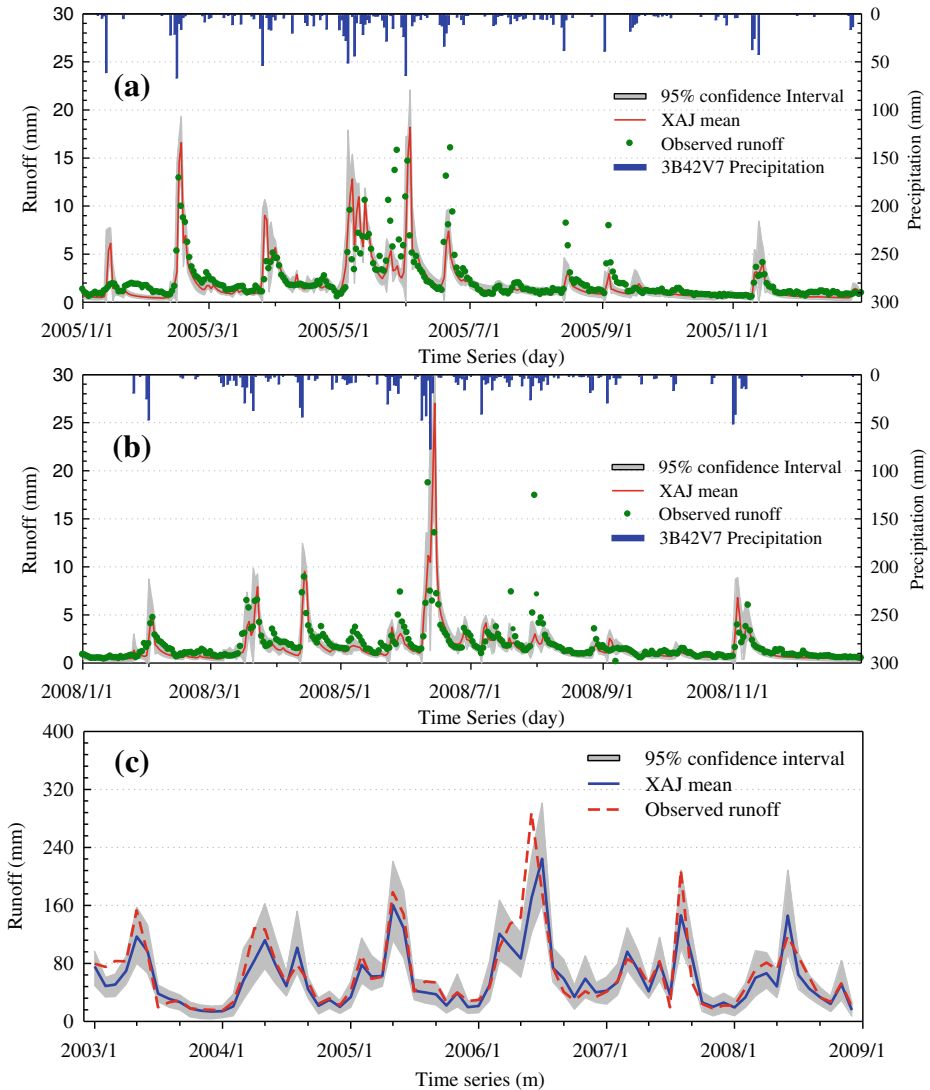
Fig. 3 XAJ model simulated runoff and calculated 95 % confidence interval based on the 3B42V7 data as input: (a) daily CP time series, (b) daily VP time series and (c) monthly time series

the simulated stream flow performances (with daily NSCE of 0.59 and 0.55, monthly NSCE of 0.87 and 0.75, BIAS of−12.06 % and−7.45 %, daily RMSE of 0.65 and 0.96 mm, and monthly RMSE of 15.10 and 28.77 mm for the calibration and validation periods, respectively) indicate that the 3B42V7 simulated stream flow captured most of the features of the observed hydrograph. The uncertainty boundary performance statistical indices (with daily CR of 61.77 % and 64.78 %, monthly CR of 88.89 % and 83.33 %, daily B of 1.37 and 1.62 mm, monthly B of 41.74 and 49.39 mm, daily D of 0.73 and 0.98 mm, and monthly D of 9.93 and 17.26 mm for the calibration and validation periods, respectively), indicate that the 3B42V7-calculated uncertainty boundary contains much information on the observed hydrograph. At the daily time scale, the simulated stream flow is in agreement with the observed hydrograph

to a certain extent, but has not captured some flood events, thus resulting in a low NSCE value. The 3B42V7 slightly underestimated rainfall (BIAS are −6.28 % and −7.02 % for the calibration and validation periods, respectively), but simulated stream flow also exhibited a certain negative BIAS. The calculated 95 % confidence interval contains more than 60 % of the observed hydrograph. At the monthly time scale, the simulated stream flow agrees well with the observed hydrograph, and it can characterize the seasonal and annual characteristics of the runoff. The calculated 95 % confidence interval contains most (more than 80 %) of the observed hydrograph.

4.2 Streamflow Simulation from 3B42RT, PERSIAN, and CMORPH

For the three real-time satellite precipitation products, we adopt the three different cases described in Section 3.1 for the stream flow simulation. Figures 4, 5, and 6 compare the BMA-combined 10,000 stream flow mean value series and calculated 95 % confidence interval with the observed hydrograph at the daily and monthly time scales in three different simulation cases. In case 1, the raw 3B42RT, PERSIAN, and CMORPH data were used as model input, and the simulated stream flow shows large underestimation compared with the observed hydrograph. The biases of the three real-time satellite precipitation products should thus be adjusted. Therefore, in cases 2 and 3, a simple precipitation error multiplier and a statistic precipitation error model were introduced to adjust the bias of the three real-time satellite precipitation products and to perform the input uncertainty analysis. The results show a significant improvement in the precision of the stream flow simulated from cases 2 and 3 compared with case 1, and the calculated 95 % confidence intervals contain most of the observed hydrograph.

Table 1 shows the statistical measures of the simulated stream flow of the three real-time satellite precipitation products and the BMA-combined stream flow during the calibration and validation periods. In case 1, the BMA-combined stream flow has low NSCE, large negative BIAS, and large RMSE for both the daily and monthly time scales, which denotes that the BMA-combined stream flow fits poorly with the observed hydrograph. The daily NSCE, BIAS and RMSE values of the case 1 BMA-combined stream flow are 0.16 (0.17), −56.42 % (−69.75 %) and 0.93 mm (1.31 mm) for the calibration (validation) period, respectively. In cases 2 and 3, the NSCE, BIAS, and RMSE values all exhibited significant improvement for both the daily and monthly time scales. The daily NSCE, BIAS and RMSE values of the case 2 BMA-combined stream flow are 0.50 (0.53), 4.78 % (1.71 %) and 0.72 mm (0.98 mm) for the calibration (validation) period, respectively. And the daily NSCE, BIAS and RMSE values of the case 3 BMA-combined stream flow are 0.58 (0.54), 0.29 % (−10.48 %) and 0.66 mm (0.98 mm) for the calibration (validation) period, respectively. Furthermore, comparing the statistical measures of the simulated stream flow of each satellite precipitation product with the results of BMA-combined stream flow, we find that in the calibration period, the BMA combination in cases 2 and 3 improve the precision of the stream flow in terms of the highest NSCE, smaller BIAS, and the smallest RMSE, whereas the BMA combinations in case 1 do not improve the precision of the stream flow owing to the weak stream flow simulation capability of PERSIAN. In the validation period, the BMA combinations in cases 2 and 3 improve the precision of the stream flow in terms of the highest NSCE and smaller BIAS and RMSE, whereas the BMA combinations in case 1 are similar to the result in the calibration period.

Table 2 shows the statistical measures of the three real-time satellite precipitation products simulated uncertainty boundary and BMA combination-calculated uncertainty boundary during the calibration and validation periods. The comparison results are similar to the precision
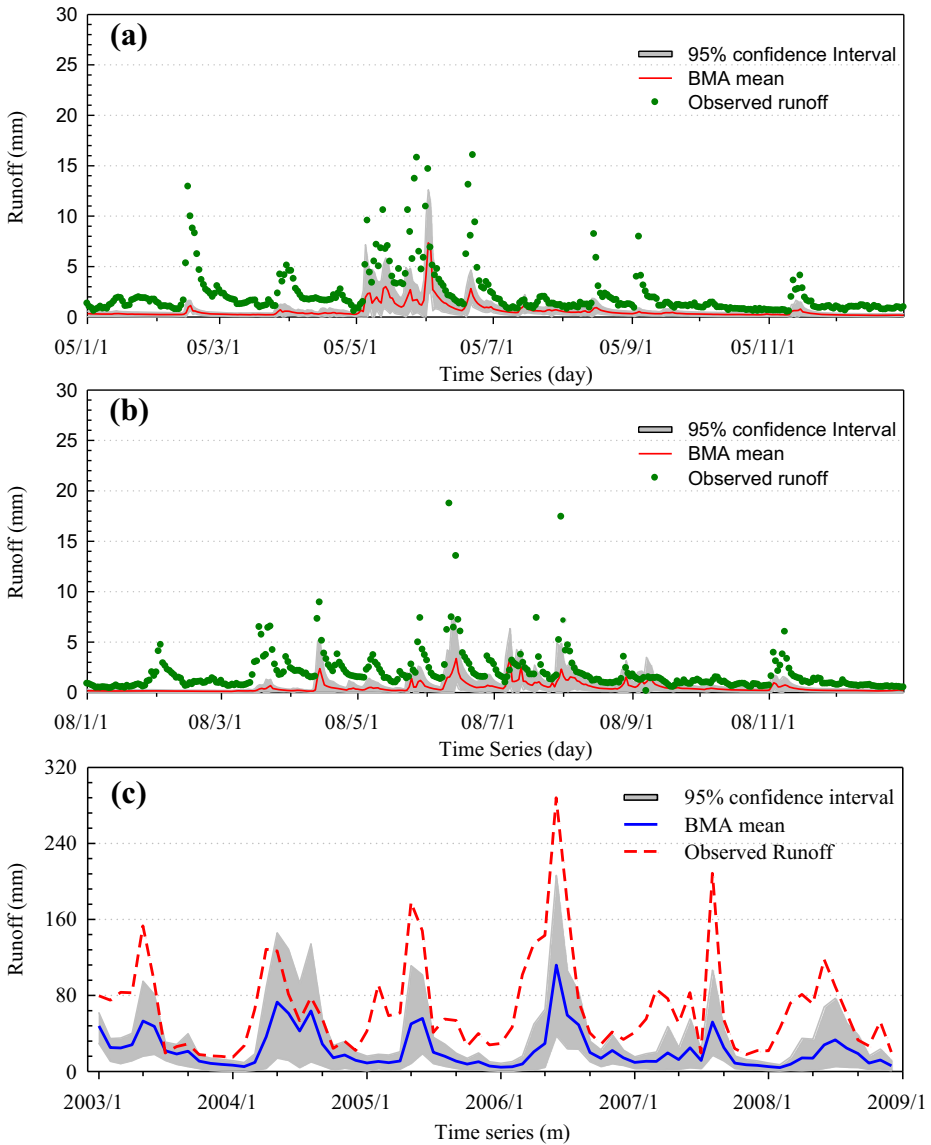
Fig. 4 XAJ model simulated runoff and calculated 95 % confidence interval based on the three real-time satellite precipitation data as input in case 1: **a** daily CP time series, **b** daily VP time series and **c** monthly time series

analysis of the stream flow. In case 1, the BMA combination-calculated 95 % confidence interval has low CR as well as large B and D for both the daily and monthly time scales, which denotes that the calculated confidence interval has weakly capability to capture the observed hydrograph. The daily CR, B and D values of the case 1 BMA combination-calculated 95 % confidence interval are 31.48 % (14.87 %), 1.31 mm (1.13 mm) and 1.24 mm (1.62 mm) for the calibration (validation) period, respectively. In cases 2 and 3, the CR, B, and D values all exhibited significant improvement for both the daily and monthly time scales. The daily CR, B
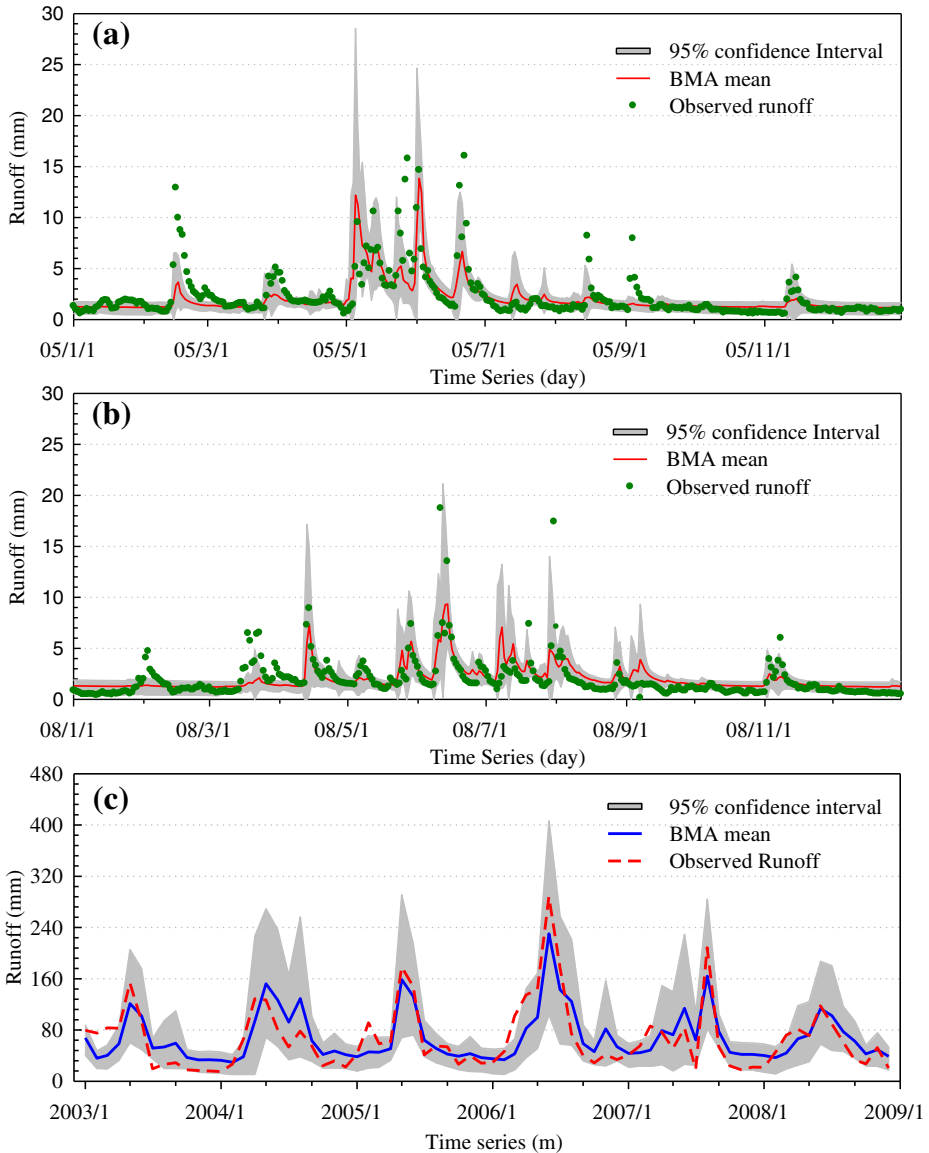
Fig. 5 XAJ model simulated runoff and calculated 95 % confidence interval based on the three real-time satellite precipitation data as input in case 2: **a** daily CP time series, **b** daily VP time series and **c** monthly time series

and D values of the case 2 BMA combination-calculated 95 % confidence interval are 65.33 % (64.87 %), 2.55 mm (2.87 mm) and 1.05 mm (1.33 mm) for the calibration (validation) period, respectively. And the daily CR, B and D values of the case 3 BMA combination-calculated 95 % confidence interval are 72.90 % (75.55 %), 2.12 mm (2.21 mm) and 0.86 mm (1.06 mm) for the calibration (validation) period, respectively. Moreover, a comparison of the statistical measures of each satellite precipitation-simulated 95 % confidence intervals with the results of BMA-combined 95 % confidence
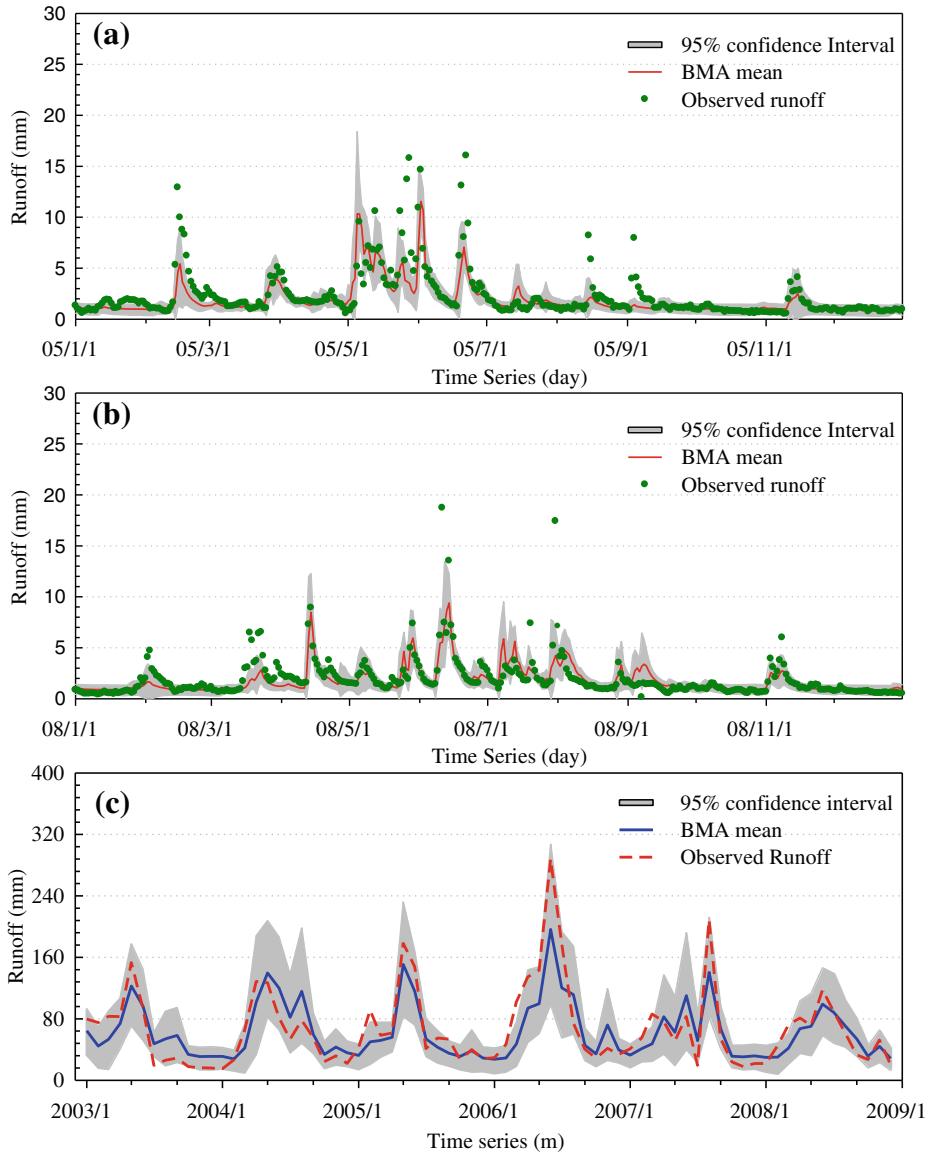
Fig. 6 XAJ model simulated runoff and calculated 95 % confidence interval based on the three real-time satellite precipitation data as input in case 3: **a** daily CP time series, **b** daily VP time series and **c** monthly time series

intervals denotes that the BMA combination can generate more skillful and reliable uncertainty boundaries than that of each satellite precipitation simulation. However, what should be noted is that the enhanced performance in the higher CR comes at the cost of a significant increase in B.

Tables 1 and 2 also display that the primarily MW-based products 3B42RT and CMORPH exhibited relatively better stream flow simulation performance than that of the primarily IR-based product PERSIAN in Mishui basin.

Table 1 Statistical measures of the three real-time satellite precipitation products simulated streamflow at three different cases

Inputs		Case 1			Case 2			Case 3		
		NSCE	BIAS (%)	RMSE (mm)	NSCE	BIAS (%)	RMSE (mm)	NSCE	BIAS (%)	RMSE (mm)
CP	3B42RT	0.11	-58.89	0.96	0.45	1.52	0.75	0.53	-3.90	0.70
	PERSIANN	-0.33	-80.21	1.17	0.39	-1.61	0.80	0.48	-0.58	0.74
	CMORPH	0.24	-48.66	0.89	0.40	14.13	0.79	0.54	5.26	0.69
	BMA (d)	0.16	-56.42	0.93	0.50	4.78	0.72	0.58	0.29	0.66
	BMA (m)	-0.29	-56.42	47.83	0.64	4.78	25.20	0.74	0.29	21.32
VP	3B42RT	0.20	-65.68	1.28	0.53	1.32	0.98	0.54	-12.19	0.98
	PERSIANN	-0.12	-83.01	1.52	0.35	10.64	1.16	0.37	-6.50	1.36
	CMORPH	0.17	-70.88	1.30	0.53	-6.42	0.99	0.52	-12.60	0.99
	BMA (d)	0.17	-69.75	1.31	0.53	1.71	0.98	0.54	-10.48	0.98
	BMA (m)	-0.30	-69.75	65.78	0.75	1.71	28.99	0.73	-10.48	29.90

4.3 Comparison of the Simulation Results

Figure 7 shows the comparison of the performance statistics of the BMA-combined three real-time satellite precipitation product simulations with the rain gauge data and 3B42V7 simulations as well as the selected indexes, including the NSCE, BIAS, and CR. By introducing a precipitation error multiplier (case 2) and a precipitation error model (case 3), recalibrated model parameters, and BMA-combined satellite precipitation product-based simulations, the precision of the simulated stream flow and the reliability of the uncertainty boundary exhibited significant improvement. At the daily time scale, the NSCE, BIAS, and CR values of simulations of cases 2 and case 3 are comparable with the results of 3B42V7 simulation. However, the precision of the satellite precipitation data-simulated stream flow is still weaker

Table 2 Statistical measures of the three real-time satellite precipitation products calculated uncertainty boundary at three different cases

| Inputs		Case 1			Case 2			Case 1		
		CR%	B (mm)	D (mm)	CR%	B (mm)	D (mm)	CR%	B (mm)	D (mm)
CP	3B42RT	21.99	0.83	1.24	55.02	1.90	1.02	54.74	1.36	0.88
	PERSIANN	7.30	0.54	1.63	51.28	1.65	1.03	54.20	1.18	0.89
	CMORPH	30.57	1.01	1.16	51.64	2.19	1.18	50.64	1.69	0.96
	BMA (d)	31.48	1.31	1.24	65.33	2.55	1.05	72.90	2.12	0.86
	BMA (m)	25.00	39.83	35.49	83.33	77.64	21.76	86.11	64.54	17.99
VP	3B42RT	16.51	0.92	1.51	57.39	2.20	1.25	65.05	1.53	1.00
	PERSIANN	8.30	0.62	1.91	43.34	2.20	1.60	54.74	1.36	1.27
	CMORPH	10.77	0.86	1.62	55.20	2.02	1.21	63.69	1.60	1.02
	BMA (d)	14.87	1.13	1.62	64.87	2.87	1.33	75.55	2.21	1.06
	BMA (m)	8.33	34.48	48.58	83.33	87.31	23.48	86.11	67.29	21.67
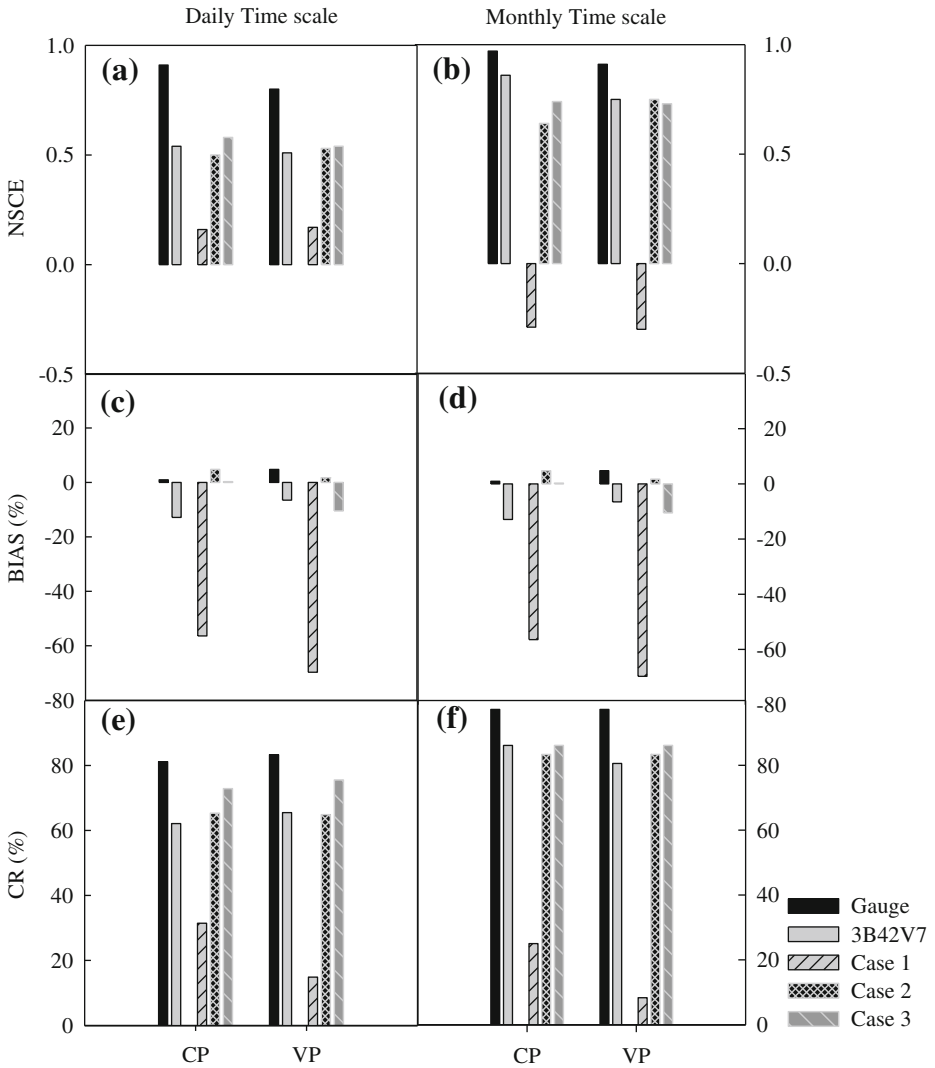
Fig. 7 Comparison of the performance statistics of the BMA-combined three real-time satellite precipitation product simulations with the gauge and 3B42V7 simulations

than the rain gauge data simulation. The accuracy of the satellite precipitation products at the daily time scale is unsatisfactory with further room for improvement. At the monthly time scale, the NSCE, BIAS, and CR values of simulations for cases 2 and 3 are comparable with the rain gauge data simulation, with an acceptable precision.

Figure 8 compares the actual evapotranspiration (AET), soil moisture (SM) and runoff calculated from the three real-time satellite precipitation products with the results simulated from the rain gauge data and 3B42V7, and the figure also gives the observed runoff value. In case 1, for the three real-time satellite precipitation products exhibit a large underestimation of rainfall, and the model parameters were calibrated based on the rain gauge data as input, the simulated AET, SM and runoff are both smaller than the
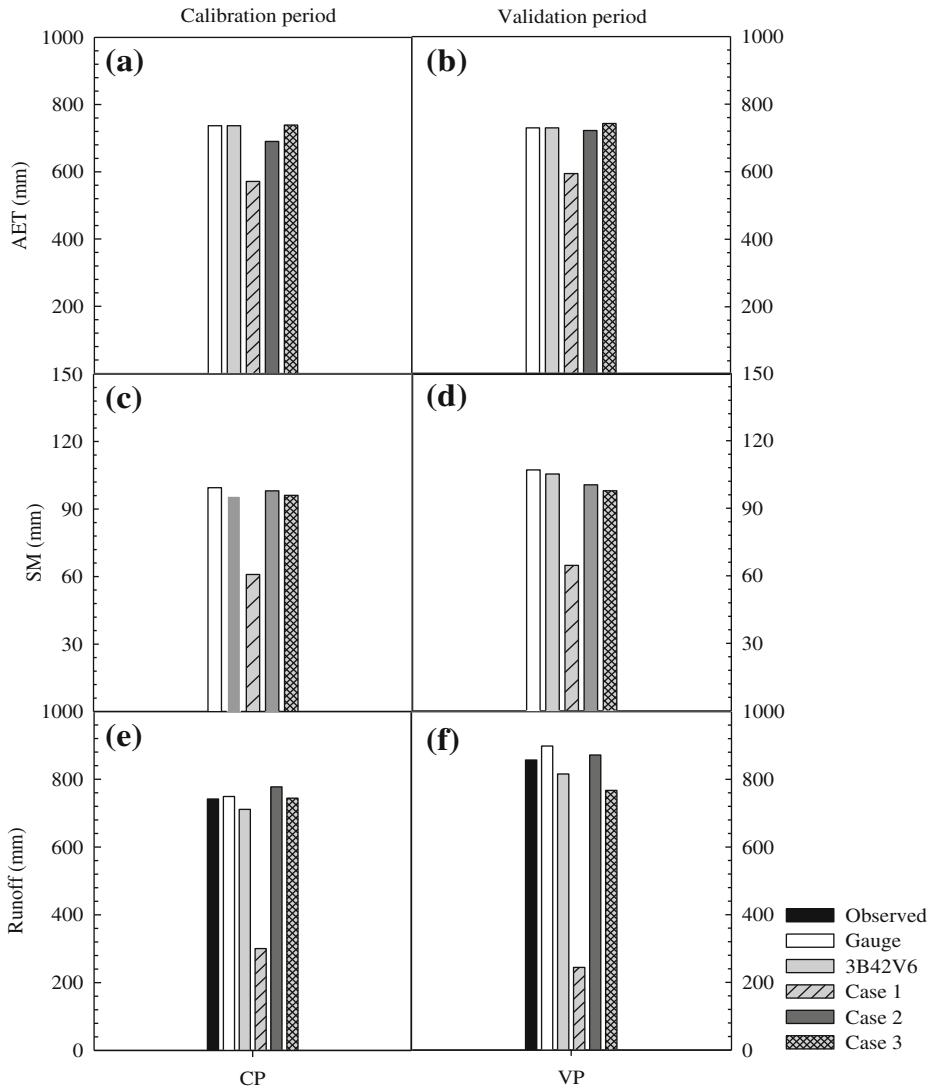
Fig. 8 Comparison of the AET, SM and runoff calculated from the three real-time satellite precipitation products with the results simulated from the rain gauge data and 3B42V7

simulations from the rain gauge data and 3B42V7. In cases 2 and 3, the biases of the three real-time satellite precipitation products were adjusted by using a precipitation error multiplier and a precipitation error model, respectively, and the model parameters were recalibrated with each of the bias-adjusted satellite precipitation products as input, the simulated AET, SM and runoff are comparable with the simulations from the rain gauge data and 3B42V7. The bias adjustment, uncertainty analysis, and BMA combination method facilitate the application of 3B42RT, PERSIAN, and CMORPH to practical applications and scientific research in such areas as water balance estimation and water resource evaluation.

5 Conclusions

Satellite precipitation products provide a new kind of input data for various hydrological models and are very important for regional and global hydrological applications, particularly for remote regions and developing countries. However, the uncertainty of currently available satellite precipitation products remains unclear, particularly for the real-time pure satellite data. Therefore, adjusting the bias of satellite precipitation products is a key step to improve their hydrological simulation utility. Furthermore, to utilize the multi-satellite precipitation products fully is another approach to achieve more reliable hydrological simulation. This study presented an integrated framework to first adjust the bias of the three real-time satellite precipitation products (i.e., 3B42RT, PERSIAN, and CMORPH) and then to perform ensemble stream flow simulation with the XAJ model and SCEM-UA algorithm in the middle-latitude Mishui basin in South China. The combined results from the three real-time pure satellite precipitation products were compared with the rain gauge data simulation and the 3B42V7 simulation results to verify the effectiveness of the proposed method. The main conclusions were drawn as follows.

The research version satellite precipitation product, i.e., 3B42V7, exhibited good performance in stream flow simulation. The calculated 95 % confidence interval contains most of the observed hydrograph. However, some minimum and maximum values run out of the interval at the daily time scale. 3B42V7 can be used for hydrological forecast and water resource estimation in ungauged and data-scarce basins. The three real-time satellite precipitation products exhibited large negative biases in terms of rainfall intensity amount. The rainfall biases directly translate to negative biases in the simulated streamflow. Therefore directly using the three real-time satellite precipitation products for streamflow simulation is not meaningful. By introducing a precipitation error multiplier and a precipitation error model to adjust the biases and by recalibrating the model parameters, the behavior of the simulated streamflow and calculated uncertainty boundary of the three real-time satellite precipitation products were significantly improved. The precipitation error multiplier method is robustly simple and easy to apply. The precipitation error model method requires the use of rain gauge data to calibrate model parameters. Thus, the method has some limitations in practical applications. Comparing the precision performance of the two error correction methods, the precipitation error model method is slightly better than precipitation error multiplier method. Finally, the BMA combination of the simulations from the three real-time satellite precipitation products can generate a significantly improved prediction and a remarkably more reliable uncertainty boundary. The proposed methodology of bias adjustment, uncertainty analysis, and BMA combination collectively facilitates the application of the real-time 3B42RT, PERSIANN, and CMORPH data to hydrological prediction, water balance estimation, and water resource evaluation over ungauged and data-scarce basins. This research is also an investigation on the hydrological utility of use of multi-satellite precipitation product input ensembles for hydrological simulation, which is potentially applicable to other regions and can integrate additional more satellite precipitation data when the Global Precipitation Measuring mission with 9-satellite constellation is anticipated in 2014.

References

Ajami NK, Duan QY, Sorooshian S (2007) An Integrated Hydrological Bayesian Multimodel Combination Framework: Confronting Input, Parameter, and Model Structural Uncertainty in Hydrologic Prediction. Water Resour Res 43, W01403

Bartier PM, Keller CP (1996) Multivariate Interpolation to Incorporate Thematic Surface Data Using Inverse Distance Weighting (IDW). Comput Geosci 22:795–799

Behrangi A, Khakbaz B, Jaw TC, AghaKouchak A, Hus K, Sorooshian S (2011) Hydrologic Evaluation of Satellite Precipitation Products Over a mid-Size Basin. J Hydrol 397(3–4):225–237

Bitew MM, Gebremichael M (2011) Evaluation of Satellite Rainfall Products Through Hydrologic Simulation in a Full Distributed Hydrologic Model. Water Resour Res 47, W06526

Duan QY, Sorooshian S, Gupta VK (1994) Optimal use of the SCE-UA Global Optimization Method for Calibrating Watershed Models. J Hydrol 158(3–4):265–284

Duan QY, Ajami NK, Gao XG, Sorooshian S (2007) Multi-Model Ensemble Hydrologic Prediction Using Bayesian Model Averaging. Adv Water Resour 30(5):1371–1386

Gottschalck J, Meng J, Rodell M, Houser P (2005) Analysis of Multiple Precipitation Products and Preliminary Assessment of Their Impact on Global Land Data Assimilation System Land Surface States. J Hydrometeorol 6(5):573–598

Gebregiorgis A, Hossain F (2011) How Much Can A Priori Hydrologic Model Predictability Help in Optimal Merging of Satellite Precipitation Products? J Hydrometeorol 12:1287–1298

Hong Y, Hsu KL, Soroosh S, Gao XG (2004) Precipitation Estimation from Remotely Sensed Imagery Using Artificial Neural Network – Cloud Classification System (PERSIANN-CCS). J Appl Meteorol 43(12):1834–1853

Hong Y, Hsu KL, Moradkhani H, Soroosh S (2006) Uncertainty Quantification of Satellite Precipitation Estimation and Monte Carlo Assessment of the Error Propagation into Hydrologic Response. Water Resour Res 42, W08421

Huffman GJ, Adler RF, Bolvin DT, Gu GJ, Nelkin EJ, Bowman KP, Hong Y, Stocker EF, Wolff DB (2007) The TRMM Multi-Satellite Precipitation Analysis (TMPA): Quasi-Global, Multi-Year, Combined-Sensor Precipitation Estimates at Fine Scales. J Hydrometeorol 8(1):38–55

Joyce RJ, Janowiak JE, Arkin PA, Xie PP (2004) CMORPH: A Method That Produces Global Precipitation Estimates from Passive Microwave and Infrared Data at High Spatial and Temporal Resolution. J Hydrometeorol 5(3):487–503

Jiang SH, Ren LL, Yong B, Yang XL, Shi L (2010) Evaluation of High-Resolution Satellite Precipitation Products With Surface Rain Gauge Observations from Laohahe Basin in Northern China. Water Sci Eng 3(4):405–417

Jiang SH, Ren LL, Hong Y, Yong B, Yang XL, Yuan F, Ma MW (2012) Comprehensive Evaluation of Multi-Satellite Precipitation Products With a Dense Rain Gauge Network and Optimally Merging Their Simulated Hydrological Flows Using the Bayesian Model Averaging Method. J Hydrol 452–453:213–225

Kubota T, Shige S, Hashizume H, Aonashi K, Takahashi N, Seto S, Takayabu YN, Ushio T, Nakagawa K, Iwanami K, Kachi M, Okamoto K (2007) Global Precipitation map Using Satellite Borne Microwave Radiometers by the GSMaP Project: Production and Validation. IEEE Trans Geosci Remote Sens 45:2259–2275

Kidd C, Huffman G (2011) Global Precipitation Measurement. Meteorol Appl 18(3):334–353

Kwon HH, Filho FAS, Block P, Sun LQ, Lall U, Jr DSR (2012) Uncertainty Assessment of Hydrologic and Climate Forecast Models in Northeastern Brazil. Hydrol Process 26(25):3875–3885

Kucera PA, Ebert EE, Turk FJ, Levizzani V, Kirschbaum D, Tapiador FJ, Loew A, Borsche M (2013) Precipitation from Space: Advancing Earth System Science. Bull Am Meteorol Soc 94(3):365–375

Li Z, Yang DW, Hong Y (2013) Multi-Scale Evaluation of High-Resolution Multi-Sensor Blended Global Precipitation Products Over the Yangtze River. J Hydrol 500:157–169

Raftery AE, Balabdaoui F, Polakowski M, Polakowski M (2005) Using Bayesian Model Averaging to Calibrate Forecast Ensembles. Mon Weather Rev 113(5):1155–1174

Sorooshian S, Hsu KL, Gao XG, Gupta HV, Imam B, Braithwaite D (2000) Evaluation of PERSIANN System Satellite-Based Estimates of Tropical Rainfall. Bull Am Meteorol Soc 81:2035–2046

Su FG, Hong Y, Lettenmaier DP (2008) Evaluation of TRMM Multi-Satellite Precipitation Analysis (TMPA) and its Utility in Hydrologic Prediction in La Plata Basin. J Hydrometeorol 9(4):622–640

Stisen S, Sandholt I (2010) Evaluation of Remote-Sensing-Based Rainfall Products Through Predictive Capability in Hydrological Runoff Modeling. Hydrol Process 24(7):879–891

Strauch M, Bernhofer C, Koide S, Volk M, Lorz C, Makeschin F (2012) Using Precipitation Data Ensemble for Uncertainty Analysis in SWAT Streamflow Simulation. J Hydrol 414–415:413–424

Vrugt JA, Gupta HV, Bouten W, Sorooshian S (2003) A Shuffled Complex Evolution Metropolis Algorithm for Optimization and Uncertainty Assessment of Hydrologic Model Parameters. Water Resour Res 39:1201

Xiong LH, Wan M, Wei XJ, Connor KM (2009) Indices for Assessing the Prediction Bounds of Hydrological Models and Application by Generalized Likelihood Uncertainty Estimation. Hydrol Sci J 54(5):852–871

Xue XW, Hong Y, Limaye AS, Gourley JJ, Huffman GJ, Shan SI, Dorji C, Chen S (2013) Statistical and Hydrological Evaluation of TRMM-Based Multi-Satellite Precipitation Analysis Over the Wangchu Basin of Bhutan: Are the Latest Satellite Precipitation Products 3B42V7 Ready for use in Ungauged Basins? J Hydrol 499:91–99

Yu MY, Chen X, Li LH, Bao AM, Paix MJ (2011) Streamflow Simulation by SWAT Using Different Precipitation Sources in Large Arid Basins With Scarce Raingauges. Water Resour Manage 25:2669–2681

Yong B, Hong Y, Ren LL, Gourley JJ, Huffman GJ, Chen X, Wang W, Khan SI (2012) Assessment of Evolving TRMM-Based Multi-Satellite Real-Time Precipitation Estimation Methods and Their Impacts on Hydrologic Prediction in a High Latitude Basin. J Geophys Res 117, D09108

Zhao RJ (1992) The Xinanjiang Model Applied in China. J Hydrol 135:371–381